PHYSICAL REVIEW D **85,** 115021 (2012)

Testing neutrino masses in the *R*-parity violating minimal supersymmetric standard model with LHC results

M. Hanussek*

Bethe Center for Theoretical Physics, University of Bonn, Bonn, Germany

J. S. Kim†

ARC Centre of Excellence for Particle Physics at the Terascale, School of Chemistry and Physics, University of Adelaide, Adelaide, Australia

(Received 2 May 2012; published 26 June 2012)

Within the *R*-parity violating minimal supersymmetric standard model, we use a hierarchical ansatz for the lepton-number violating trilinear Yukawa couplings by relating them to the corresponding Higgs-Yukawa couplings. This ansatz reduces the number of free parameters in the lepton-number violating sector from 36 to 6. Baryon-number violating terms are forbidden by imposing the discrete gauge symmetry baryon triality. We fit the lepton-number violating parameters to the most recent neutrino oscillation data, including the mixing angle θ_{13} found by Daya Bay. We find that we obtain phenomenologically viable neutrino masses and mixings only in the case of normal ordered neutrino masses and that the lepton-number violating sector is unambiguously determined by neutrino oscillation data. We discuss the resulting collider signals for the case of a neutralino as well as a scalar tau lightest supersymmetric particle. We use the ATLAS searches for multijet events and large transverse missing momentum in the 0, 1, and 2 lepton channel with 7 TeV center-of-mass energy in order to derive exclusion limits on the parameter space of this *R*-parity violating supersymmetric model.

DOI: 10.1103/PhysRevD.85.115021 PACS numbers: 12.60.Jv, 14.60.Pq, 14.80.Ly

I. INTRODUCTION

A main objective of both multi-purpose experiments ATLAS and CMS at the Large Hadron Collider (LHC) is the search for new physics beyond the standard model (SM). Many of these extensions, in particular supersymmetry (SUSY) [1,2], include new heavy colored states and a weakly interacting lightest new particle escaping detection. Thus the most generic signal among these models are several hard jets and large transverse missing momentum ($\not{p}_T$). ATLAS and CMS grouped their multijet and missing transverse momentum searches into 0, 1, 2 lepton studies [3–14], in order to be sensitive to different SUSY models and to avoid an overlap between these studies. Most studies were recently updated to the full data set of about 5 fb^{-1} recorded in 2011 at a center-of-mass energy of 7 TeV. So far, no excess above SM expectations has been observed, and strict bounds on any supersymmetric model or another relevant new physics model providing a similar collider signal can be derived. ATLAS and CMS mainly concentrate on SUSY searches which are based on *R*-parity conserving (R_p) supersymmetric extensions of the SM [15]. An equally well motivated scenario is a *R*-parity violating ($\not{R}_p$) supersymmetric SM [16], where the discrete symmetry baryon triality (B_3) [17] is imposed in order to avoid baryon-number violation and proton decay. The particle spectrum is the same as for R_p models. However, lepton (*L*-) number is violated and the lightest supersymmetric particle (LSP) is not stable any more. Thus an alternative dark matter candidate may be needed such as the axino or gravitino [18,19]. In principle, any supersymmetric particle can now be the lightest supersymmetric particle (LSP) [20]. The LSP decays lead to observable effects at the LHC, which can be significantly different from models with *R*-parity conservation [21,22]. Also, the *L*-violation causes massive neutrinos to emerge in the B_3 minimal supersymmetric SM (MSSM) [23–26] without introducing a new seesaw mass scale or extending the particle spectrum [27,28]. Data from neutrino experiments can be used to constrain the *L*-violating couplings [24].

Within the B_3 MSSM, we make a hierarchical ansatz in the *L*-violating sector, relating the trilinear *L*-violating Yukawa couplings to the Higgs-Yukawa couplings, as first proposed in Ref. [26]. This reduces the number of free *L*-violating parameters to six. We take into account experimental results on neutrino oscillations, which amounts to five constraints (neutrino mixing angles and mass-squared differences). When additionally fixing the overall neutrino mass scale, this enables us to unambiguously determine the magnitude of the six *L*-violating parameters, removing all degrees of freedom from the *L*-violating sector.

Consequently, the decay properties of the LSP in the hierarchical B_3 MSSM depend only on the experimental neutrino data. We expect no difference in the production and decay chains of supersymmetric particles compared to the R_p MSSM, since the magnitude of the *L*-violating

*hanussek@th.physik.uni-bonn.de
†jongsoo.kim@adelaide.edu.au

couplings needs to be fairly small (of order 10^{-5}) in order to be in accordance with neutrino data.

There have been several ATLAS and CMS searches as well as phenomenological studies for $\not{R}_p$ models, based on resonant slepton production, multilepton signatures or displaced vertices [29–35]. However, most of these studies constrain models where the L-violating couplings are either very large (for single slepton production), very small (for displaced vertices), or where we have single coupling dominance and four body decays (4 lepton signature) [36]. Neither of these criteria is the case in most regions of the hierarchical B_3 MSSM parameter space. Apart from these studies, the results of the ATLAS 1 lepton, multijet and $\not{p}_T$ study with 1 fb^{-1} of data were used to restrict a bilinear R-parity violating model [37], which takes into account constraints from neutrino data [9].

In this study, we would like to reinterpret the ATLAS studies with jets, $\not{p}_T$ and 0, 1, or 2 isolated leptons [3,9,12] in the light of the hierarchical B_3 MSSM. Except for the 2 lepton study, which uses 1 fb^{-1}, the studies have been updated to 5 fb^{-1} [5,10], using the full 2011 data. Since in a generic B_3 MSSM, the number of free parameters in the SUSY breaking sector is too large to perform a systematic study, we work in the B_3 constrained MSSM (B_3 cMSSM) [38], which imposes simplifying assumptions on the scalar and gaugino masses and couplings at the unified (GUT) scale. It turns out that only specific regions of the cMSSM parameter space are phenomenologically viable when taking into account neutrino data [24], and we focus on these parameter regions. As a result, there are four free parameters in the SUSY breaking sector besides the six L-violating parameters.

In Sec. II, we shortly discuss how neutrino masses are generated in the hierarchical B_3 cMSSM. We then describe how we fit the L-violating parameters in order to obtain the correct masses and mixing angles of the neutrino sector at any parameter point in the hierarchical B_3 cMSSM parameter space. In Sec. III, we examine the arising collider signatures for the case of stau LSP and neutralino LSP scenarios. In Sec. IV, we present bounds on the hierarchical B_3 cSSM neutrino model derived from SUSY ATLAS searches. We conclude in Sec. V.

II. HIERARCHICAL BARYON TRIALITY CMSSM AND MASSIVE NEUTRINOS

A. Hierarchical baryon triality (B_3) cMSSM

The B_3 MSSM allows for additional, L-violating terms in the superpotential compared to the R_p MSSM [39–41],

$$\mathcal{W}_{B_3} = \mathcal{W}_{R_p} + \epsilon_{ab}[\tfrac{1}{2}\lambda_{ijk}L_i^a L_j^b \bar{E}_k + \lambda'_{ijk}L_i^a Q_j^b \bar{D}_k - \kappa_i L_i^a H_u^b]. \quad (1)$$

L_i, Q_i correspond to the SU(2) doublet lepton and quark superfields. $\bar{E}_i$, $\bar{D}_i$ are the SU(2) singlet lepton and down-type quark superfields, respectively. $i, j, k \in \{1, 2, 3\}$ are generation indices, $a, b \in \{1, 2\}$ ($\epsilon_{12} = 1$) are indices of the $SU(2)_L$ fundamental representation, while the corresponding $SU(3)_c$ indices are suppressed. The trilinear couplings λ_{ijk} correspond to nine independent parameters due to the antisymmetry of the first two indices i, j, whereas the trilinear couplings λ'_{ijk} denote 27 independent parameters. The bilinear couplings κ_i are 3 dimensionful couplings.

For universal supersymmetry breaking, the bilinear L-violating couplings and the corresponding soft-breaking terms can be simultaneously rotated to zero at the GUT scale via a basis transformation of the lepton and Higgs superfields [38,42]. However, nonvanishing κ_i terms (and nonaligned soft-breaking terms) are generated at the electroweak (EW) scale via the renormalization group equations (RGEs) [43].

In the B_3 cMSSM, the number of free parameters in the soft-breaking sector is constrained. We end up with $5 + n$ independent parameters at the GUT scale [38],

$$M_0, \quad M_{1/2}, \quad A_0, \quad \mathrm{sgn}(\mu), \quad \tan\beta, \quad \Lambda. \quad (2)$$

M_0, $M_{1/2}$, and A_0 denote the universal scalar mass, universal gaugino mass, and universal trilinear scalar coupling, respectively. $\mathrm{sgn}(\mu)$ is the sign of the superpotential Higgs mixing parameter and $\tan\beta$ is the ratio between the two Higgs VEVs. Λ denotes a subset of n independent dimensionless trilinear L-violating couplings.

In this work, we further restrict the number of free L-violating parameters: In the B_3 cMSSM, the down-type Higgs superfield and the SU(2) doublet lepton superfield have the same gauge quantum numbers [44]. They are indistinguishable because lepton number is broken. Thus, the L-violating trilinear terms in Eq. (1) resemble terms in the R-parity conserving superpotential,

$$\mathcal{W}_{R_p} \supset \epsilon_{ab}[(Y_E)_{jk}H_d^a L_j^b \bar{E}_k + (Y_D)_{jk}H_d^a Q_j^b \bar{D}_k], \quad (3)$$

where $(Y_E)_{jk}$ and $(Y_D)_{jk}$ are the Higgs-Yukawa couplings of the lepton and the down-type quarks, respectively. We therefore proposed the following ansatz at the GUT scale [26], which can be motivated in the framework of Froggatt-Nielsen models [42]

$$\lambda_{ijk} \equiv \ell_i \cdot (Y_E)_{jk} - \ell_j \cdot (Y_E)_{ik}, \quad (4)$$

$$\lambda'_{ijk} \equiv \ell'_i \cdot (Y_D)_{jk}. \quad (5)$$

Here, ℓ_i, ℓ'_i are c-numbers. Eq. (4) has the required form to maintain the antisymmetry of the λ_{ijk} in the first two indices. Assuming a specific form of the Higgs-Yukawa couplings, the number of L-violating parameters reduces to six complex numbers. We have given our ansatz in the weak-current basis. However, after EW symmetry breaking, we must rotate to the mass-eigenstate basis. Experimentally, only the Pontecorvo-Maki-Nakagawa-Sakata and the Cabibbo-Kobayashi-Maskawa matrices are known [45,46]. The explicit lepton and quark mixing

matrices are therefore not fully determined. In the following, we assume that the lepton Higgs-Yukawa matrix is diagonal. Thus, we assume mixing only in the neutrino sector for the leptonic sector. In the quark sector, we assume left-right symmetric mixing. Additionally, we work in the limit where the down-type Higgs-Yukawa matrix is diagonal whereas the up-type is nondiagonal. Hence our specific form of the Higgs-Yukawa couplings implies mixing only in the up-type sector. In Ref. [25], it was shown that the choice of quark mixing (e.g. mixing in the up-type versus mixing in the down-type sector) does not significantly influence the numerical results at the low energy scale.

B. B_3 neutrino masses

Since lepton number is violated, the neutrinos mix with the neutralinos, resulting in a 7×7 neutralino-neutrino mass matrix of rank 5. As a result, we obtain one massive neutrino at tree level [38],

$$m_\nu^{\text{tree}} = -\frac{16\pi\alpha_{\text{GUT}}}{5}\frac{\sum_{i=1}^{3}(v_i - v_d\frac{\kappa_i}{\mu})^2}{M_{1/2}}. \tag{6}$$

Here v_d, v_u, and v_i denote the vacuum expectation values of the H_d, H_u, and sneutrino fields. However, experimental neutrino oscillation data suggests that we need at least two massive neutrinos. Since there is only one massive neutrino at tree level, higher-order corrections need to be taken into account. Full 1-loop corrections to the neutrino-neutralino mass matrix have been discussed in Ref. [25]. A good estimate of the size of these radiative corrections is given by the slepton-lepton and down-type quark-squark loop contribution, which are proportional to [47]

$$(m_\nu^\ell)_{ij} \propto \lambda_{ikn}\lambda_{jnk}m_{\ell_k}m_{\ell_n}, \tag{7}$$

$$(m_\nu^d)_{ij} \propto N_c\lambda'_{ikn}\lambda'_{jnk}m_{d_k}m_{d_n}. \tag{8}$$

The proportionality of the loop contributions to the exchanged SM fermion mass in the loop further increases the effect that trilinear couplings with indices $i33$ are dominant over all other indices ijk, as is clear from the hierarchical ansatz in Eqs. (4) and (5).

Reference [24] noted that in large regions of cMSSM parameter space the ratio between the tree-level neutrino mass and the radiative contributions is too large to yield a phenomenologically viable neutrino mass hierarchy. However, due to RGE effects in the running of L-violating parameters, the tree-level neutrino mass has a global minimum at

$$A_0^{(\lambda')} \approx 2M_{1/2}, \tag{9}$$

$$A_0^{(\lambda)} \approx \frac{M_{1/2}}{2}, \tag{10}$$

for nonzero λ'_{ijk} or λ_{ijk}, respectively. We choose A_0 such that it minimizes the λ' contribution to neutrino masses [Eq. (9)], as explained in more detail in the next paragraph. Thus, in the hierarchical B_3 cMSSM a set of 10 free parameters,

$$M_{1/2}, \quad M_0, \quad \text{sgn}(\mu), \quad \tan\beta, \quad \ell_i, \quad \ell'_i, \tag{11}$$

fixes the full B_3 cMSSM.

As described in Ref. [25], it is possible to obtain the experimentally measured neutrino mass squared differences and mixing angles by independently generating each neutrino mass with a set of three L-violating free parameters. This means that 6 or 9 independent couplings are necessary in order to obtain the full spectrum with either two or three massive neutrinos. However, in the case of neutrinos in normal hierarchy mass ordering with a massless lightest neutrino, it turns out that one can do with only two couplings to explain the heaviest neutrino mass, m_{ν_3}, cf. Ref. [25]. This is fortunate, because due to our hierarchical ansatz only ℓ'_i, ℓ_1, and ℓ_2 have a significant impact on the neutrino sector whereas ℓ_3 generates only a negligible contribution to the neutrino masses if it is of the same order of magnitude as the other couplings [48]. Therefore, we generate m_{ν_3} at tree level via the λ_{ijk} couplings, which are in turn determined by ℓ_1 and ℓ_2. The second neutrino mass, m_{ν_2} is generated via λ'_{ijk} (determined by the ℓ'_i) at the 1-loop level, whereas the lightest neutrino must remain massless, $m_{\nu_1} \approx 0$.

In summary, we have five free L-violating parameters which control the neutrino sector, ℓ'_i and ℓ_1, ℓ_2. These can be used to generate nonzero m_{ν_2} and m_{ν_3}, respectively, in accordance with the two mass squared difference and three mixing angles from experiment. It is not easily possible to obtain inverse hierarchy or degenerate neutrino masses in the hierarchical B_3 cMSSM unless ℓ_3 becomes several orders of magnitude larger than the other L-violating parameters.

C. Experimental neutrino oscillation data

Assuming three active oscillating neutrinos, the best global fit values of the neutrino masses and mixing parameters at 1σ confidence levels (C.L.) are given by [49,50],

$$\begin{aligned}
\sin^2[\theta_{12}] &= 0.31 \pm 0.02, \\
\sin^2[\theta_{23}] &= 0.51 \pm 0.06, \\
\sin^2[2\theta_{13}] &= 0.09 \pm 0.02, \\
\Delta m_{21}^2 &= 7.59 \pm 0.2 \times 10^{-5}\text{eV}^2, \\
\Delta m_{31}^2 &= \left\{ \begin{array}{c} -2.34 \pm 0.1 \times 10^{-3}\text{eV}^2 \\ 2.45 \pm 0.1 \times 10^{-3}\text{eV}^2 \end{array} \right\}
\end{aligned} \tag{12}$$

where

$$\Delta m_{ij}^2 \equiv m_{\nu_i}^2 - m_{\nu_j}^2. \tag{13}$$

m_{ν_i} denote the neutrino masses in order of largest electron-neutrino admixture. There are two large mixing angles θ_{12} and θ_{23}. Deviating from Ref [49], we use in Eq. (12) for θ_{13} the best fit value recently measured by Daya Bay and RENO [50,51]. The neutrino oscillation data implies at least two nonvanishing neutrino masses m_{ν_i}. In this work, we usually consider the so-called normal hierarchy (NH) scenario, where $\Delta m^2_{31} > 0$ and $m_{\nu_1} \approx 0$.

D. Numerical results

For each cMSSM point, we fit the L-violating parameters ℓ_i and ℓ'_i to the best-fit normal hierarchy neutrino mass data in Eq. (11). We perform this fit by minimizing the χ^2 function

$$\chi^2 = \frac{1}{N_{\rm obs}} \sum_{i=1}^{N_{\rm obs}} \left(\frac{f_i^{\rm softsusy} - f_i^{\rm obs}}{\delta_i} \right), \tag{14}$$

where $f_i^{\rm obs}$ are the central values of the $N_{\rm obs}$ experimental observables in Eq. (12), $f_i^{\rm softsusy}$ are the corresponding numerical predictions and δ_i are the 1σ uncertainties. We calculate the low energy mass spectrum and couplings with SOFTSUSY3.3.0 [52]. The numerical minimization of our χ^2 function is done with the program package MINUIT2 [53]. Details of our numerical procedure can be found in Ref. [25]. Here, we present an example solution where we translate the best fit values ℓ_i and ℓ'_i into the corresponding values of the trilinear L-violating couplings at the unification scale:

$$\begin{aligned} \lambda_{133} &= 1.72 \times 10^{-6} \qquad \lambda_{233} = 2.74 \times 10^{-6} \\ \lambda'_{133} &= 1.13 \times 10^{-5} \qquad \lambda'_{233} = 3.89 \times 10^{-5} \\ \lambda'_{333} &= 3.11 \times 10^{-5}. \end{aligned} \tag{15}$$

We have used $M_0 = 100$ GeV, $M_{1/2} = 500$ GeV, $\tan\beta = 25$, $\mathrm{sgn}(\mu)$, and $A_0^{(\lambda')} \approx 2M_{1/2}$. As one can see, the λ_{i33} and λ'_{i33} couplings are between $\mathcal{O}(10^{-5})$ and $\mathcal{O}(10^{-6})$. All remaining trilinear L-violating couplings are at least one order of magnitude smaller, below $\mathcal{O}(10^{-7})$. The couplings λ'_{233} and λ'_{333} tend to be the largest trilinear L-violating couplings. In Fig. 1, we display the best fit value of λ'_{233} in the $M_0 - M_{1/2}$ plane. We see that the magnitude of the L-violating couplings does not strongly depend on M_0 and $M_{1/2}$. Furthermore, the relative magnitude of the L-violating couplings to each other remains roughly the same throughout the parameter space.

Recall that the parameter ℓ_3 is not fixed by the neutrino oscillation data in the normal hierarchy scenario. However, we assume that ℓ_3 is of the same order of magnitude as ℓ_1 and ℓ_2, setting $\ell_3 = \ell_2$ in the rest of our paper [54].

We have checked all low energy constraints on the L-violating trilinear couplings [55,56]. However, in our case the couplings are too small to have an observable impact on any low energy observables.

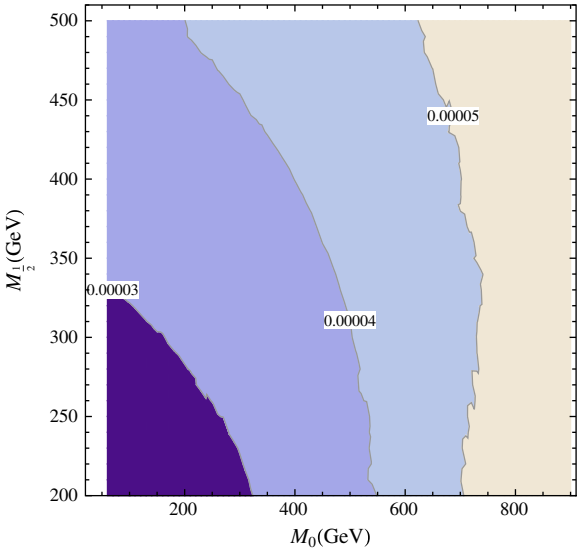

FIG. 1 (color online). Best-fit values of the L-violating coupling λ'_{233} at the unification scale in the M_0–$M_{1/2}$ plane, fixing $A_0^{(\lambda')} \approx 2M_{1/2}$, $\tan\beta = 25$ and $\mathrm{sgn}(\mu) = +1$.

III. COLLIDER SIGNATURES

In this section, we investigate possible collider signatures of the hierarchical B_3 cMSSM at the LHC. The best-fit values of the L-violating couplings to neutrino data are too small to have an observable effect on the resonant production of supersymmetric particles. Thus, pair production of colored sparticles via strong interactions is the dominant production channel at the LHC. Only if sleptons and gauginos are much lighter than the colored sparticles, their production rate becomes comparable. The produced sparticles cascade decay into the LSP. In our parameter space, we can have either a stau LSP or a neutralino LSP [57]. The final state collider signature is determined by the decay properties of the LSP candidate. In the B_3 cMSSM, the LSP is almost always short-lived and decays within the detector via the L-violating interactions [58]. We now describe the final state signatures of stau LSP and neutralino LSP scenarios separately after describing the numerical tools used. Then we go on to discuss in which regions of $M_0 - M_{1/2}$ parameter space they occur.

A. Numerical tools

The low energy mass spectrum and couplings are calculated with SOFTSUSY3.3 [52]. The decay widths of the relevant sparticles are obtained with ISAJET7.64 [59] and ISAWIG1.200. However, the decay channels of the neutralino LSP via the sneutrino VEVs and the κ_i term are absent in ISAWIG1.200. Therefore, we calculate decays via the bilinear L-violating couplings with SPHENO3.1 [60]. We combined all decay widths in order to calculate the branching ratio of the sparticles. We use the parton distribution functions MRST2007 LO modified [61]. Our signal events are

generated with HERWIG6.510 [62]. The cross sections are normalized with the next-to-leading order calculations from PROSPINO2.1 [63] assuming equal renormalization and factorization scale. Our events are stored in the Monte Carlo event record format STDHEP5.6.1. We take into account detector effects by using the fast detector simulation DELPHES1.9 [64], where we choose the default ATLAS-like detector settings. Our event samples are then analyzed with the program package ROOT [65] and we calculate the 95% and 68% C.L. of the exclusion limits with TRolke [66].

B. Stau LSP decay

In the parameter region where the lighter stau $\tilde{\tau}_1$ is the LSP, pair produced squarks and gluinos at the LHC cascade decay into the LSP, producing jets and taus (tau-neutrinos) along the way,

$$pp \to \tilde{q}\,\tilde{q}\,/\tilde{q}\,\tilde{g}\,/\tilde{g}\,\tilde{g} \to \tilde{\tau}_1\tilde{\tau}_1 + 2j + X, \tag{16}$$

where j and X denote jets and additional particles of the process (such as τ or ν_τ), respectively. Note that we can have more than 2 jets in the final state if the process involves gluinos. These additional jets are included in X, which we discuss in more detail in Sec. III D. For example, right-handed squarks decay into a jet and the lightest neutralino, which then typically decays into a stau and a tau with a branching ratio of one,

$$\tilde{q}_R\tilde{q}_R \to jj\tilde{\chi}_1^0\tilde{\chi}_1^0 \to jj\tau\tau\tilde{\tau}_1\tilde{\tau}_1. \tag{17}$$

The stau then directly decays into two SM fermions via the trilinear L-violating couplings λ_{133}, λ_{233}, and λ'_{3jk}, cf. Fig 2. Decays via the λ_{i33} couplings are dominant, even though the decay width via λ'_{3jk} is enhanced by a factor of $N_C = 3$ and the λ'_{3jk} couplings are generally larger. However, the lightest stau is mostly right-handed and thus the coupling of the stau via λ' is suppressed due to the small admixture with the left-handed stau. Additionally, the stau decay via λ'_{333} into a top and bottom quark is kinematically forbidden or suppressed in large regions of parameter space. Stau decays via λ'_{311} and λ'_{322} are heavily suppressed due to the smallness of the couplings.

In principle, the stau can also mix with the charged Higgs boson via κ_3 and decay via the two-body decay mode $\tilde{\tau} \to \tau\nu$. However, we have numerically checked that stau decays via bilinear operators are always subdominant in our model. We define a

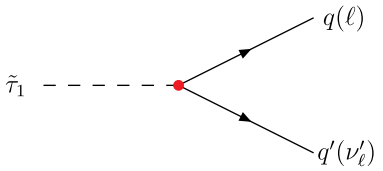

FIG. 2 (color online). Schematic characterization of the stau LSP decay in the hierarchical B_3 cMSSM.

(i) *benchmark point BP1* in the stau LSP region with

$$M_0 = 100\ \text{GeV}, \qquad M_{1/2} = 500\ \text{GeV},$$
$$\tan\beta = 25, \qquad \text{sgn}(\mu) = 1 \quad \text{and} \quad A_0^{(\lambda')} \approx 2M_{1/2}$$

This benchmark point is characterized by lightest neutralino, lighter stau, gluino and squark masses of 205 GeV, 162 GeV, 1146 GeV, and 1012 GeV, respectively. The dominant LSP branching ratios for **BP1** are given by

$$\begin{aligned} \text{Br}(\tilde{\tau}_1^- \to \tau^-\nu_e) &= 0.26 \\ \text{Br}(\tilde{\tau}_1^- \to \tau^-\nu_\mu) &= 0.21 \\ \text{Br}(\tilde{\tau}_1^- \to e^-\nu_\tau) &= 0.26 \\ \text{Br}(\tilde{\tau}_1^- \to \mu^-\nu_\tau) &= 0.21 \\ \text{Br}(\tilde{\tau}_1^- \to s\bar{c}) &= 0.04. \end{aligned} \tag{18}$$

Note that the branching ratios into different decay channels are roughly independent of the stau mass as long as the final state masses are negligible.

Roughly half of the staus decay into a charged lepton and neutrino, the other half decays into a tau and neutrino. Note that we only denote electrons or muons as leptons in this paper. Since one third of taus decay leptonically, we expect final state collider signatures with either 0, 1, or 2 leptons from the decaying stau LSPs, for 12%, 46%, and 42% of events, respectively:

$$\begin{aligned} &0\ell + 2\nu + 2\tau_{\text{had}} + 2j + X \\ &1\ell + 2(4)\nu + 1\tau_{\text{had}} + 2j + X \\ &2\ell + 2(4,6)\nu + 2j + X \end{aligned} \tag{19}$$

where ℓ denotes an electron or muon and τ_{had} denotes a hadronically decaying tau. If the lepton[s] in the 1ℓ or 2ℓ channel come from a leptonically decaying tau, the number of neutrinos increases from 2 to 4 [6], as shown in brackets in Eq. (19). Due to the Majorana character of the neutralino, both neutralinos can decay into like-charged staus and hence we can have same-sign leptons in the final state.

C. Neutralino LSP decay

In the hierarchical B_3 cMSSM, the lightest neutralino eigenstate is generally bino-like. The production process is given by

$$pp \to \tilde{q}\,\tilde{q}\,/\tilde{q}\,\tilde{g}\,/\tilde{g}\,\tilde{g} \to \tilde{\chi}_1^0\tilde{\chi}_1^0 + 2j + X. \tag{20}$$

The neutralino LSP can either decay via a trilinear L-violating operator into three SM fermions or via neutralino-neutrino mixing (proportional to the bilinear L-violating couplings and the sneutrino VEVs) into a gauge/Higgs boson and a lepton, cf. Fig. 3.

For relatively low sfermion masses in the propagator, the trilinear three-body decay modes dominate because the

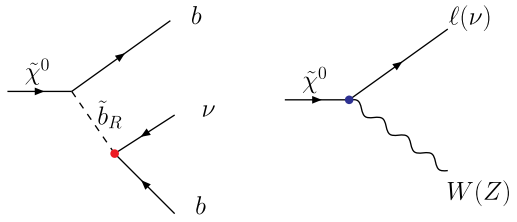

FIG. 3 (color online). Schematic characterization of the three-body (left) and two-body (right) decay modes of the neutralino LSP in the hierarchical B_3 cMSSM.

bilinear L-violating couplings are only generated radiatively via RGE running and the sneutrino VEVs are determined to be relatively small from radiative EW symmetry breaking. However, in parameter regions with heavy sfermions, the bilinear two-body decay mode becomes dominant because the three-body decay mode suffers from phase space suppression and heavy virtual sfermions in the propagator.

First, we discuss the case where the lightest neutralino dominantly decays via the trilinear L-violating couplings, for which we define

(i) *benchmark point* **BP2** with

$$M_0 = 200\ \text{GeV}, \qquad M_{1/2} = 400\ \text{GeV},$$
$$\tan\beta = 25, \qquad \text{sgn}(\mu) = 1 \quad \text{and} \quad A_0^{(\lambda')} \approx 2M_{1/2}$$

This benchmark point is characterized by lightest neutralino, lighter stau, gaugino, and squark masses of 163 GeV, 213 GeV, 937 GeV, and 846 GeV, respectively. We obtain the following LSP branching ratios for **BP2**:

$$\begin{aligned}
\text{Br}(\tilde{\chi}_1^0 \to {}^{(-)}_{\ell}\nu b\bar{b}) &= 0.31 \\
\text{Br}(\tilde{\chi}_1^0 \to {}^{(-)}_{\tau}\nu b\bar{b}) &= 0.20 \\
\text{Br}(\tilde{\chi}_1^0 \to W^{\pm}\ell^{\mp}) &= 0.21 \\
\text{Br}(\tilde{\chi}_1^0 \to W^{\pm}\tau^{\mp}) &= 0.05 \\
\text{Br}(\tilde{\chi}_1^0 \to {}^{(-)}_{\tau}\nu Z^0) &= 0.13 \\
\text{Br}(\tilde{\chi}_1^0 \to {}^{(-)}_{\tau}\nu h^0) &= 0.08
\end{aligned} \tag{21}$$

The branching ratio of the three-body decay modes (the $\tilde{\chi}_1^0 \to \nu b\bar{b}$ channel) is roughly 51%. However, for this benchmark point the two-body L-violating decays via bilinear L-violating couplings already have a sizable contribution to the LSP decays. The electron (electron-neutrino) channel is suppressed compared to the muon decay channel because $\lambda'_{133} \sim 0.3\lambda'_{233}$, cf. Eq. (15). Therefore, about 90% of our leptons are muons. Summing up the various decay channels and including the gauge boson branching ratios, roughly 72% of neutralinos decay without leptons, 19% with one lepton, and 7% with two leptons. This leads to 52%, 27%, and 14% of events with 0, 1, and 2 leptons from LSP decays, respectively.

Assuming the cascade decay processes of Eq. (20), dominant final state signatures are then given by

$$\begin{aligned}
&0\ell + 2\nu + 2b\bar{b} + 2j + X \\
&1\ell + 1\nu + b\bar{b} + W_{\text{had}} + 2j + X \\
&2\ell + 2\nu + b\bar{b} + 2j + X
\end{aligned} \tag{22}$$

Next, we discuss the decay properties of the lightest neutralino in a region where the two-body decays dominate,

(ii) *benchmark point* **BP3** with

$$M_0 = 600\ \text{GeV}, \qquad M_{1/2} = 400\ \text{GeV},$$
$$\tan\beta = 25, \qquad \text{sgn}(\mu) = 1 \quad \text{and} \quad A_0^{(\lambda')} \approx 2M_{1/2}$$

The lightest neutralino, lighter stau, gluino, and squark masses of **BP2** are 164 GeV, 579 GeV, 961 GeV, and 1010 GeV, respectively. Here, the LSP decay channels are the same as for **BP2**; however, the branching ratios differ drastically:

$$\begin{aligned}
\text{Br}(\tilde{\chi}_1^0 \to {}^{(-)}_{\ell}b\bar{b}) &= 0.04 \\
\text{Br}(\tilde{\chi}_1^0 \to {}^{(-)}_{\tau}b\bar{b}) &= 0.03 \\
\text{Br}(\tilde{\chi}_1^0 \to W^{\pm}\ell^{\mp}) &= 0.40 \\
\text{Br}(\tilde{\chi}_1^0 \to W^{\pm}\tau^{\mp}) &= 0.14 \\
\text{Br}(\tilde{\chi}_1^0 \to {}^{(-)}_{\tau}Z^0) &= 0.27 \\
\text{Br}(\tilde{\chi}_1^0 \to {}^{(-)}_{\tau}h^0) &= 0.12
\end{aligned} \tag{23}$$

Since here the scalar masses (M_0) are fairly large, the two-body neutralino decay modes via bilinear L-violating couplings or sneutrino VEVs dominate, amounting to 93%. Therefore, there are only half as many neutralinos decaying into the 0ℓ channel as for **BP2**; twice as many decay into the 1ℓ and 2ℓ channel. This results in final state signatures with 0,1, or 2 leptons at 24%, 37%, and 27%, respectively. Typical final state signatures are given by

$$\begin{aligned}
&0\ell + 2\nu + 2Z^0_{\text{had}/\nu\nu} + 2j + X \\
&1\ell + 1\nu + Z^0_{\text{had}/\nu\nu} + W_{\text{had}} + 2j + X \\
&2\ell + 2\nu + Z^0_{\text{had}/\nu\nu} + 2j + X
\end{aligned} \tag{24}$$

As mentioned before, the electron decay channel is suppressed by roughly a factor of 10 compared to the muon decay channel. Additionally to the channels mentioned in Eq. (24), there are 12% of events with 3 or 4 leptons from LSP decay.

D. Scan in the M_0–$M_{1/2}$ plane and kinematical distributions

In the subsequent numerical analysis, we perform a scan in the M_0–$M_{1/2}$ plane. For this, we define a benchmark region (**BR**) which contains the three benchmark points defined above (**BP1**, **BP2**, **BP3**):

(i) *benchmark region* **BR** (where M_0, $M_{1/2}$ free):

$$\tan\beta = 25, \qquad \mathrm{sgn}(\mu) = 1 \quad \text{and} \quad A_0^{(\lambda')} \approx 2M_{1/2}$$

BP1, **BP2**, and **BP3** each lie in distinct sections of the BR: stau LSP region, neutralino LSP region dominated by three-body decays, and neutralino LSP region dominated by two-body decays, respectively. This is depicted in Fig 4, where the ratio between three-and two-body decay modes of the neutralino LSP is displayed. The two-body $\tilde{\chi}_1^0$ decay modes dominate at large $M_{1/2}$ and M_0. As one can also see in this figure, the stau LSP region within our **BR** is approximately given by

$$M_{1/2} \geq 3M_0 - 80\ \mathrm{GeV}, \tag{25}$$

since the lightest neutralino mass is driven to larger values by the large $M_{1/2}$. In general, the lighter stau mass eigenstate is mostly right-handed.

In Sec. II B, we discussed that the absolute magnitude of the L-violating parameters as well as the relative magnitude between them does not vary significantly with M_0 and $M_{1/2}$. This implies that the LSP decay branching ratios are hardly affected by variations of the L-violating parameters within our **BR**. However, the decay modes are importantly affected by two points, as illustrated in Fig. 4:

(A) Whether we are in the stau or neutralino LSP region

(B) The ratio between three- and two-body decay modes within the neutralino LSP region.

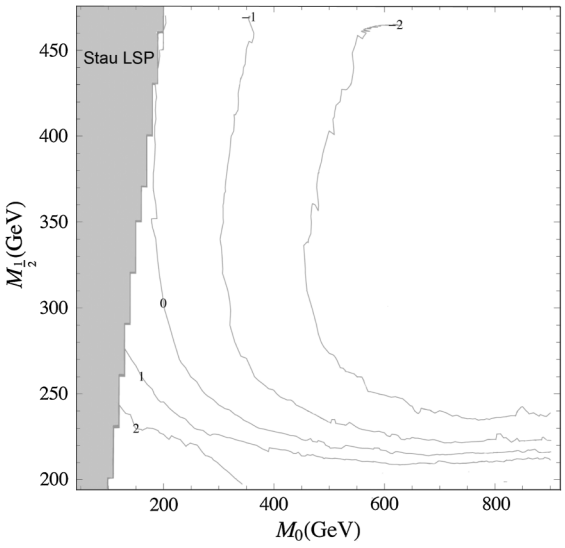

FIG. 4. The iso curves show the logarithmic ratio between three-body and two-body decay modes of the neutralino LSP in our benchmark region. In the stau LSP region, the two-body stau decay modes via the trilinear RPV couplings are always dominant.

In the stau LSP region, the 1 and 2 lepton channels are dominant for large regions of parameter space. The 0 lepton channel only becomes significant once the stau becomes heavier than the top-quark. Then, hadronic stau decays via λ'_{i33} contribute significantly and the 1 and 2 lepton studies perform much worse, resulting in a "cutoff" of the sensitive region for stau masses above the top mass. Now, the 0 lepton channel could further exclude parameter space; however, since this region extends well above $M_{1/2} \approx 500$ GeV, we expect that the amount of data collected is not yet large enough to make exclusion possible. In the neutralino LSP region dominated by three-body decays, we expect the 0 lepton channel to be the best, whereas in the case of two-body decays, the 2 lepton channel should perform better.

We now come to a discussion of possible additions to the final state particles from "X" [as contained in Eqs. (16) and (20)] and the most important distributions for our benchmark region.

Additional jets can arise from gluinos in the hard process, since the gluino decays into quark and (virtual) squark, leading to more jets in the final state [67]. Besides gluino pair and gluino-squark production, gluinos can occur in squark decays if $M_{1/2} \ll M_0$. For example, in **BP3** the gluinos are lighter than the squarks and a sizable fraction of the squarks decay into a gluino and a quark which then decays via virtual squark and quark. Thus, we expect a higher jet multiplicity than for **BP1** or **BP2**, where $m_{\tilde{q}} < m_{\tilde{g}}$. This is illustrated in Fig. 5(a). There, we show the distribution of the number of jets for our three benchmark points as well as for a R_p-conserving version of **BP2** and **BP3** with a stable LSP (denoted "**BP2 RPC**" and "**BP3 RPC**," respectively). One can see that for **BP2 RPC**, there are on average only 2–3 jets because here squarks typically decay into a neutralino/chargino and a quark, whereas for **BP3 RPC**, there are 3–4 jets. Comparing **BP2 RPC** to **BP2**, we expect up to 4 additional b-jets from the neutralino LSP decays [Eq. (22)], and thus the distribution peaks around $N_{\mathrm{jet}} = 5$–6, cf. Fig. 5(a). Similar observations can be made for **BP3**. Here, there are more jets from the (R-parity conserving) decay chain involving gluinos. However, on average there are less jets from neutralino LSP decays, Eq. (24), such that the distribution also peaks at $N_{\mathrm{jet}} = 5$–6. In the stau LSP case (**BP1**), the distribution peaks at $N_{\mathrm{jet}} = 3$–4. Here there are only few jets which can be attributed to X (ie. gluino decays), as discussed above.

Further leptons in the final state can emerge in the cascade decays of the SU(2) doublet squarks. The latter decay into charginos and neutralinos with dominant SU(2)

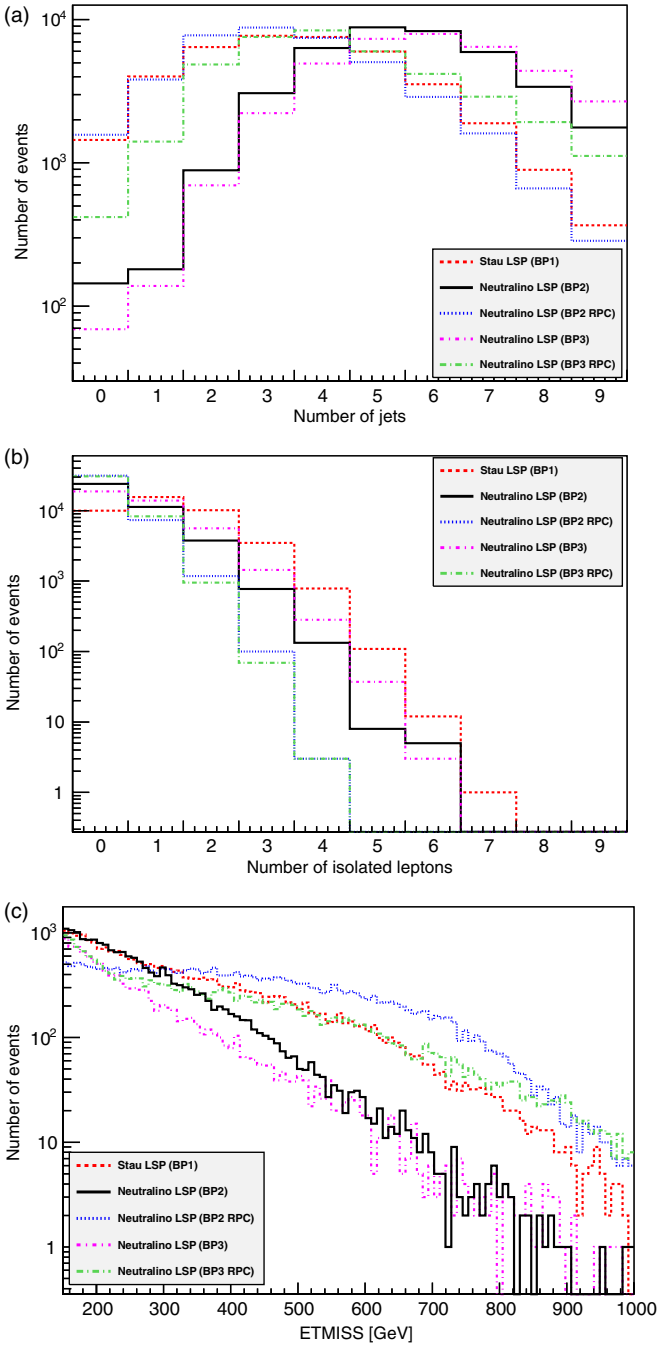

FIG. 5 (color online). We depict (a) the number of jets N_{jet}, (b) the number of isolated leptons N_ℓ with $p_T > 20$ GeV and (c) the missing transverse momentum ("ETMISS") for our benchmark points **BP1**, **BP2** and **BP3**. Additionally we display an R_p version of **BP2** and **BP3** ("**BP2 RPC**", "**BP3 RPC**"), where the neutralino LSP is kept stable. We generated 40 000 events for each benchmark point.

gaugino composition, which are typically $\tilde{\chi}_1^\pm$ and $\tilde{\chi}_2^0$ in the cMSSM. $\tilde{\chi}_1^\pm$ and $\tilde{\chi}_2^0$ subsequently decay either into slepton and lepton or gauge boson/Higgs and the lightest neutralino. However, this leads to isolated leptons in only $\sim$15% of events in our case, as is illustrated in Fig. 5(b) by the N_ℓ distributions for **BP2 RPC** and **BP3 RPC**. The reason for this is that in **BP2**, the $\tilde{\tau}_1$ is much lighter than the other sleptons, whereas the latter are heavier than $\tilde{\chi}_2^0$ and $\tilde{\chi}_1^\pm$. Thus $\tilde{\chi}_2^0$ and $\tilde{\chi}_1^\pm$ dominantly decay into $\tilde{\tau}\tau$ and $\tilde{\tau}\nu$, respectively. About one third of these τ's decay leptonically, leading to final state leptons. In **BP3**, all sleptons are heavier than $\tilde{\chi}_1^\pm$ and $\tilde{\chi}_2^0$ and hence the latter preferably decay into a gauge/Higgs boson and the lightest neutralino. Comparing **BP2 RPC** and **BP3 RPC** with the corresponding $\not{R}_p$ scenarios, we clearly see that there are significantly more leptons for **BP2** and **BP3** due to leptonic decays of $\tilde{\chi}_1^0$. However, there are more entries in the 0 lepton bin for **BP2** and **BP3** than expected from Eqs. (22) and (24), because some of the leptons are nonisolated or too soft or do not fall into the acceptance region of the tracking system. The same holds for **BP1**, which has overall the largest number of isolated leptons; nevertheless the ratio between events with 1 lepton and 0 leptons is still less than predicted from Eq. (19).

In Fig. 5(c), we present the missing transverse momentum distribution. Here, we clearly see that **BP1** has the hardest distribution among all R_p violating distributions. Note that for the two other R_p violating scenarios the missing transverse energy distribution is much softer compared to the respective R_p conserving scenarios, due to the LSP decays.

IV. NUMERICAL RESULTS: EXCLUSION LIMITS ON HIERARCHICAL B_3 CMSSM PARAMETER SPACE

In this section, we further constrain the hierarchical B_3 cMSSM parameter space using data from the LHC at $\sqrt{s} = 7$ TeV with an integrated luminosity of up to 5 fb^{-1}. We focus on recent ATLAS studies with 0,1, or 2 isolated leptons, several jets, and large missing transverse momentum. A short overview over the ATLAS studies used is given in Table I. Full details of objects reconstruction, definitions of all kinematical observables, and event selection cuts of all three analyses can be found in the respective ATLAS publications [3–5] (0 lepton), [9,10] (1 lepton), and [12] (2 leptons). We have chosen these analyses because they only rely on simple objects such as electrons, muons, jets, and missing transverse momentum in the final state. Thus, we do not rely on complicated tau reconstruction and b-tagging algorithms, which are difficult to simulate with the detector simulation DELPHES1.9 [64]. In particular, difficulties arise in reconstructing hadronically decaying taus [21]. Also, the published ATLAS studies for supersymmetry involving taus [68] or b-jets [69] in the final states have smaller cross-sections or smaller efficiencies than the multijet, large $\not{p}_T$ and lepton searches. Thus, we expect the "simple" 0–2 lepton analyses to perform better with the current amount of data. So far, the experimental data is in agreement with the SM background expectations. We use their results in order to derive the

TABLE I. The main cuts used in the ATLAS studies used in this collider study. More details concerning the cuts can be found in the relevant ATLAS studies (0 lepton [5], 1 lepton [10], and 2 lepton [12]). N_ℓ denotes the number of isolated leptons, $N_{\rm jet}$ the number of jets, and $p^T_{\rm jets}$ specifies the minimal transverse momentum which is required for these jets. $\not{p}_T$ gives the minimal value of missing transverse momentum of the event, $m^{\rm (inc)}_{\rm eff}$ the minimal (inclusive) effective mass, and $\mathcal{L}$ denotes the total integrated luminosity at 7 TeV.

	0lept-SRE-m	1lept-3j	2lept-OS-4j
N_ℓ	0	1	2
$N_{\rm jet}$	6	3	≥ 4
$p^T_{\rm jets}$	$>(130, 60, 60, 60, 40, 40)$	$>(100, 25, 25)$	$>(100, 70, 70, 70)$
$\not{p}_T$	>160	>250	>100
$m^{\rm inc}_{\rm eff}$	>1200	>1200	...
$\frac{\not{p}_T}{m_{\rm eff}}$	>0.15	>0.3	...
$\mathcal{L}$	4.7 fb^{-1}	4.7 fb^{-1}	1.0 fb^{-1}

68% and 95% C.L. exclusion regions in the M_0–$M_{1/2}$ parameter space. We plan to investigate exclusion limits arising from third generation studies and multilepton studies in a future publication.

ATLAS and CMS have recently published conference notes which found that the lightest Higgs is at least heavier than 117.5 GeV at 95% C.L. [70,71]. In the hierarchical B_3 cMSSM, the lightest Higgs is typically rather lighter than 116 GeV, because the value of A_0 is necessarily fixed to be positive and similar in magnitude to $2M_{1/2}$, cf. Sec. II B. This means that the stop mixing cannot become very large and thus the loop contributions to the lightest Higgs mass are moderate. We have checked various values of $\tan\beta$ and both $\mathrm{sgn}(\mu) = \pm 1$; however, we found that the Higgs mass does not become larger than 117 GeV for M_0, $M_{1/2} < 1$ TeV. Therefore, the exclusion limits derived from this lightest Higgs mass bound would by far exceed the exclusion limits derived from the 0, 1, and 2 lepton channels mentioned above. However, it could be possible to soften the bound if we extend the field content of the hierarchical B_3 MSSM by a singlet, i.e., working in the next-to minimal supersymmetric standard model [72–74]. We leave this topic for a future investigation at a time when there is more certainty regarding the lightest Higgs mass.

Before applying the model independent cross section limits from the ATLAS searches to our neutrino model, we checked that the Monte Carlo tools are correctly tuned. Therefore, we generated 20 000 events for each grid point in the M_0–$M_{1/2}$ plane in the R-parity conserving cMSSM. We determined the 95% C.L. exclusion region in the M_0–$M_{1/2}$ plane for the ATLAS "1lepton-3j" study (cf. Table I) and verified that our results are compatible with the interpretation from ATLAS within ± 30 GeV. We now discuss the 0, 1, and 2 lepton channels in detail.

A. 0 lepton channel

ATLAS has used the 0 lepton channel as one of the first search channels for supersymmetry [3–5]. So far, they have collected a total luminosity of about 4.7 fb^{-1} at the center-of-mass energy of $\sqrt{s} = 7$ TeV. From the nonobservation of an excess, we can derive exclusion limits on the hierarchical B_3 cMSSM. The ATLAS 0 lepton channel is divided into several signal regions (SR). For all signal regions, the cut on $\not{p}_T$ and the minimum requirement on $p^T_{\rm jet}$ of the first two most-energetic jets are identical. However, the number of jets and the minimum $p^T_{\rm jet}$ cut for the remaining jets as well as the cut on $m^{\rm inc}_{\rm eff}$ and on the ratio $\not{p}_T/m_{\rm eff}$ differ for the different signal regions.

We have examined all signal regions after applying the object reconstruction described in their study and found that we obtain the strictest exclusion limits for the "SRE-m" signal region, which demands six jets, $m^{\rm incl}_{\rm eff} > 1200$ GeV and $\frac{\not{p}_T}{m_{\rm eff}} > 0.15$, cf. Table I. We show the resulting plot in the M_0–$M_{1/2}$ plane in Fig. 6. The exclusion limit peaks at $M_0 \approx 200$ GeV. This is the region where the neutralino LSP decays dominantly via three-body decays $\tilde{\chi}^0_1 \to \nu b\bar{b}$, *c. f.* Fig. 4. It was to be expected that the "SRE-m" signal region gives good exclusion limits for this type of scenario, because if both neutralinos decay via $\tilde{\chi}^0_1 \to \nu b\bar{b}$, we expect at least six parton level jets

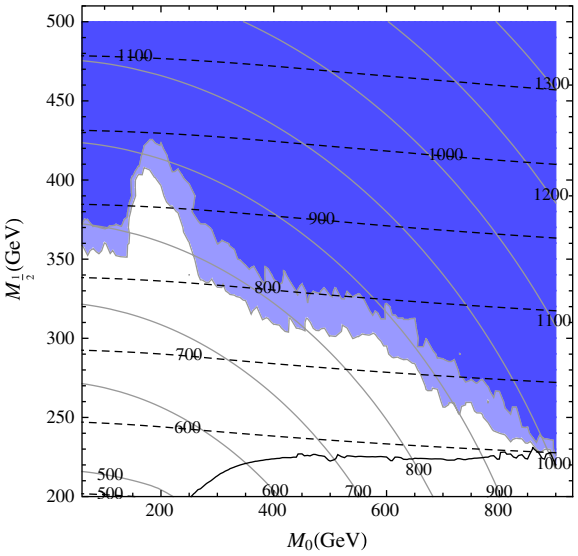

FIG. 6 (color online). Exclusion limit on our benchmark region, where $\tan\beta = 25$, $\mathrm{sgn}(\mu) = 1$ and $A_0^{(\lambda')} \approx 2M_{1/2}$, from the 0 isolated leptons, 6-jets and MET ("0lept-SRE-m") ATLAS study. The white region is excluded at 95% C.L., the light blue is excluded at 68% C.L. The grey lines denote the gluino masses, the dashed black lines denote the squark masses (each in GeV). The black line delineates the region (below) where the lifetime of the LSP becomes larger than $c\tau \gtrsim 15$ mm. In this region, the exclusion limits are not applicable because the ATLAS study rejects leptons and jets which do not originate from the primary vertex.

(including b-jets). Also, we have only moderate $\not{p}_T$ because of the three-body decay of the neutralino, and therefore more events survive in the "SRE-m" than in the "SRE-t" scenario (where $m_{\text{eff}}^{\text{inc}} > 1500$ GeV). Finally, leptons from the cascade decays of SU(2) doublet squarks into $\tilde{\chi}_1^{\pm}$ and $\tilde{\chi}_0^2$ are suppressed, since the latter dominantly decay into $\tilde{\chi}_1^{\pm} \to \tilde{\tau}\nu$ and $\tilde{\chi}_2^0 \to \tilde{\tau}\tau$.

For increasing M_0, the exclusion region decreases to lower $M_{1/2}$ values. We can see in Fig. 4 that the two-body decay mode of the neutralino becomes more important here. Thus, an increasing number of the neutralino LSPs decay into a gauge boson and a lepton and less b-jets are expected in the final state, so that less events pass the kinematical cuts on the final state jets. Another effect is that for larger M_0, the production cross section decreases.

Directly to the left of the peak at $M_0 \approx 200$ GeV, the limit drops off sharply because here the LSP becomes the $\tilde{\tau}_1$ and there are significantly less events with six jets and no leptons. However, $M_{1/2} \lesssim 350$ GeV can still be excluded at 95% C.L. We would like to point out that in principle, it is possible to obtain better exclusion limits (up to $M_{1/2} \lesssim 400$ GeV) in the stau LSP case by using a signal region with only four or five jets. However, the 1 lepton study performs even better and therefore we go not into detail about the results from these signal regions here.

We do not consider the region with a LSP lifetime exceeding $c\tau = 15$ mm, since the ATLAS searches for supersymmetry require prompt LSP decays. In Fig. 6, the region below the solid black curve highlights a LSP with a lifetime $c\tau \geq 15$ mm.

B. 1 lepton channel

References [9,10] search for multijet events with large missing transverse momentum and exactly one isolated lepton. Similarly to the 0 lepton channel in the previous subsection, the 1 lepton channel was one of the first supersymmetry search channels and the current integrated luminosity is 4.7 fb^{-1} at the center-of-mass energy of 7 TeV. They consider signal regions with 3- or 4-jets with different kinematic configurations, which are optimized for the R_p cMSSM with a large mass difference between the gluino and the LSP. Additionally, they include a soft-lepton signal region which is sensitive to scenarios with small mass splitting between the sparticles.

Comparing the results for the different signal regions, we observe that the 3-jet signal region ("1lept-3j") provides us with the best overall exclusion limits in the stau LSP region up to $M_{1/2} \sim 500$ GeV (i.e., better than the limits from any other signal region in the 0 to 2 lepton channels). The main kinematic cuts of the 1lept-3j signal region are listed in Table I and the resulting plot is shown in Fig. 7. Almost half of the events in the stau LSP region decay into final states with 1 lepton, cf. Sec. III B. Note also that the 1 lepton study [10] demands the most stringent cut on $\not{p}_T$ among the 0, 1, and 2 lepton studies. In the stau

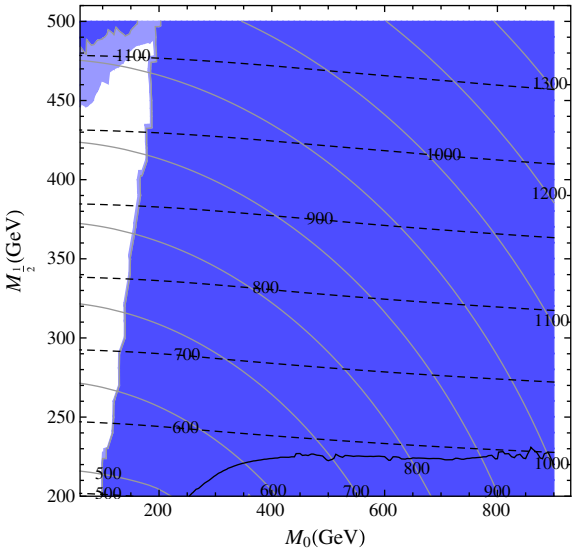

FIG. 7 (color online). Exclusion limit on our benchmark region, where $\tan\beta = 25$, $\text{sgn}(\mu) = 1$ and $A_0^{(\lambda')} \approx 2M_{1/2}$, from the 1 isolated lepton, 3-jets and MET ("1lept-3j") ATLAS study [10]. The white region is excluded at 95% C.L., the light blue is excluded at 68% C.L. The grey lines denote the gluino masses, the dashed black lines denote the squark masses (each in GeV). The black line delineates the region (below) where the lifetime of the LSP becomes larger than $c\tau \gtrsim 15$ mm. In this region, the exclusion limits are not applicable because the ATLAS study rejects leptons and jets which do not originate from the primary vertex.

LSP region with direct (two-body) leptonic decays, much more missing transverse momentum is produced than in the neutralino LSP region. In particular in the neutralino LSP region with dominant three-body decays into $\nu\bar{b}b$, the amount of $\not{p}_T$ is greatly reduced compared to the stau LSP region. Moreover, much less charged leptons arise from the neutralino decay. Additional leptons from the cascade decays are also heavily suppressed. Thus, we have a sharp drop of the acceptance in the crossover region between the stau and neutralino LSP region. For larger M_0 values, eventually the two-body neutralino decay modes become dominant over the three-body decay mode. However, the hard cut on $\not{p}_T$ still rejects many signal events in this region.

Note that the ATLAS signal region with 1 lepton and 4-jets is also sensitive to the neutralino LSP region besides the stau LSP region. This explains why in the old 4-jet signal region with 1 fb^{-1} in the muon channel, ATLAS was able to constrain the bilinear $\not{R}_p$ model presented in Ref. [9] (with two-body neutralino decays) quite well. However, having in mind that in our case we have additional three-body decays and in the new 5 fb^{-1} study, the cuts are more stringent cuts than the 1 fb^{-1} version and not optimized for our type of scenario, the resulting exclusion limits on the neutralino LSP region are weaker than the limits derived in the 2 lepton channel as shown below.

C. 2 lepton channel

The ATLAS study based on final states with two leptons and missing transverse momentum [12] has not yet been updated to include more than 1 fb^{-1} of data. The search is divided into opposite-sign (OS), same-sign (SS), and flavor-subtraction (FS) signal regions where up to four jets are demanded besides exactly two leptons and a cut on $\not{p}_T$. We find that we obtain the best exclusion limits with the OS signal regions. The three OS regions differ in the $\not{p}_T$ cut, the number of jets, and the corresponding minimal p^T_{jets} cut. As in the case of the 1 lepton channel, the OS studies with the hardest transverse missing momentum cut ("2lept-OS-2j", $\not{p}_T > 250$ GeV) are quite sensitive to the stau LSP region where two staus decay leptonically. However, in the 2 lepton channel the obtained exclusion limits are ~50 GeV weaker than in the "1lept-3j" study. This is due to the stringent cuts on $m^{\text{inc}}_{\text{eff}}$ and on the ratio $\not{p}_T/m_{\text{eff}}$ in the "1lept-3j" search channel, which yield better signal isolation and background suppression.

The OS and 4-jet channel with a moderate $\not{p}_T$ cut of 100 GEV ("2lept-OS-4j"), described in Table I, provides us with the best exclusion limits for $M_0 \gtrsim 300$ GeV, where the neutralino LSP decays dominantly via two-body decays as shown in Fig. 8. We notice a slight dip for smaller M_0 ($M_0 \sim 200$ GeV), where there are dominant three-body neutralino decays. Here, as discussed in the previous subsections, parton-level leptons from the neutralino LSP decays or from the cascade decays of the SU(2) doublet squarks are heavily suppressed and the exclusion limits from the 0 lepton channel are more stringent. For even smaller values of M_0, we are in the stau LSP region and the exclusion limits improve again. However, as discussed in the last paragraph, the cuts are not optimized for a stau LSP scenario. The E^{miss}_T cut is the weakest among all three analyses in Table I and the kinematic requirements on the jets are harder compared to the "1lept-3j" search channel.

For $M_0 \gg M_{1/2}$, the gluino is generally lighter than the squarks and thus we expect a higher jet multiplicity and in general more jets passing the kinematic cuts. However, much less transverse momentum is generated compared to the R-parity conserving case or the stau LSP region. Thus, the "2lept-OS-4j" yields the better overall exclusion region in the neutralino LSP region with dominant bilinear RPV decays due to the softer E^{miss}_T cut compared to "0lept-SREm". One further remark on the number of leptons in the final state: for $M_{1/2} \ll M_0$, the SU(2) doublet squarks decay via a winolike gaugino is quite sizable, although we have the competing decay channel via an off-shell gluino. These winolike gauginos again dominantly decay into gauge bosons providing additional leptons in the final state.

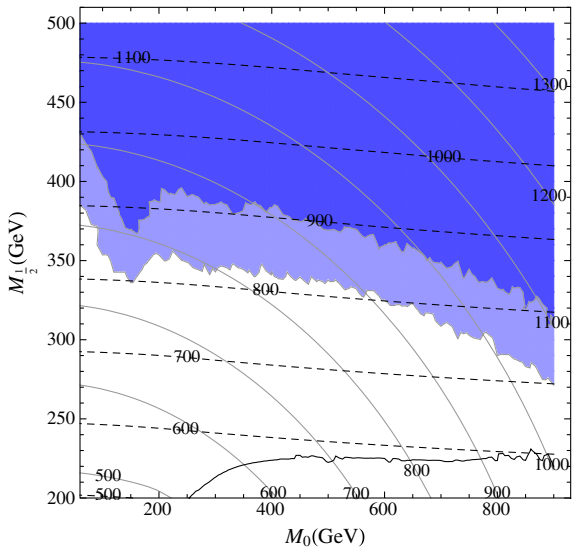

FIG. 8 (color online). Exclusion limit on our benchmark region, where $\tan\beta = 25$, $\text{sgn}(\mu) = 1$, and $A_0^{(\lambda')} \approx 2M_{1/2}$, from the 2 isolated opposite-sign leptons, 4-jets and MET ("2lept-OS-4j") ATLAS study. The white region is excluded at 95% C.L., the light blue is excluded at 68% C.L. The grey lines denote the gluino masses, the dashed black lines denote the squark masses (each in GeV). The black line delineates the region (below) where the lifetime of the LSP becomes larger than $c\tau \gtrsim 15$ mm. In this region, the exclusion limits are not applicable because the ATLAS study rejects leptons and jets which do not originate from the primary vertex.

V. SUMMARY AND CONCLUSION

We introduced a hierarchical ansatz for the L-violating trilinear Yukawa couplings in the B_3 cMSSM. Here, the trilinear L-violating Yukawa couplings are related to the Higgs Yukawa couplings via six independent parameters ℓ_i and ℓ'_i. We have then determined the best fit values of the ℓ_i and ℓ'_i in order to obtain phenomenologically viable neutrino masses and mixing angles. It is possible to quasi unambiguously determine the L-violating sector as well as the value of the SUSY breaking scalar coupling A_0 from neutrino oscillation data. We discussed the final collider signatures in the stau LSP and neutralino LSP scenarios at the LHC and finally used the ATLAS searches in jets and large missing transverse momentum with 0, 1, and 2 isolated leptons in order to find the 95% and 68% C.L. exclusion limits in the M_0–$M_{1/2}$ plane for fixed $\text{sgn}(\mu)$ and $\tan\beta$. We can exclude squark masses below 800 GeV, and gluino masses below 700 GeV (for squark masses below 1 TeV) at 95%. These limits become more stringent at 68% C.L., by roughly 100 GeV. Compared to the case of the R-parity conserving cMSSM, we obtain weaker limits because generally we have more jets and leptons and less $\not{p}_T$ due to the LSP decays.

We want to conclude with a short discussion of how we can improve a future collider study for our model or similar R-parity violating models. There are a number of studies in which R-parity violating collider signatures are investigated, as mentioned in the introduction. Many of these

studies consider multilepton ($N_\ell \geq 3$) signatures in association with much less missing transverse energy than in our study. They typically assume, however, a single nonzero λ_{ijk} without third generation indices, i.e. $i, j, k \in \{1, 2\}$, so that the number of lepton is enhanced. In our model, the LSP dominantly decays via λ_{i33} or λ'_{i33} couplings involving third generation decay products, or via neutralino-neutrino mixing involving gauge boson decay products. However, the branching ratio of the LSP into leptons is still considerably large (between 19% and 47%) and therefore the lepton multiplicity is higher than in R-parity conserving models. Also, the average p_ℓ^T distribution of the signal leptons will be relatively hard due to the large phase space of the two body decay channels of the LSP into SM fermions. For example, in **BP2** the hardest lepton has on average $p_\ell^T = 80$ GeV. In **BP2 RPC**, the hardest lepton has a mean value of $p_\ell^T = 60$ GeV. Demanding one (two) lepton(s) with moderate p_ℓ^T cuts might be advantageous to isolate the signal. As an alternative, we can also apply a kinematical cut on the scalar sum of all the leptons' p_ℓ^T.

Decays via trilinear couplings with third generation indices are dominant in large regions of parameter space in our model. Therefore, we expect a substantial proportion of events with third generation SM particles in this parameter region. For example, we expect a large number of taus and b-jets in **BC1** and **BC2**, respectively. In **BP2**, about 50% of all events have at least one b-jet. This is in sharp contrast to **BP2 RPC** where only 13% of all events have a b-jet in the final state. Requiring hadronically decaying taus or b-jets in the final state should help to suppress the SM background. However, for the parameter region around **BP3**, the LSP dominantly decays via neutralino-neutrino mixing. Here, we do not expect third generation particles in the final state in abundance.

The increase in jet and lepton multiplicities due to LSP decays in our model happens at the cost of less missing transverse momentum compared to the R-parity conserving case. For example, in **BP3 RPC** we have on average $\not{p}_T = 213$ GeV because the stable neutralino LSP escapes detection. In **BP3** we obtain a mean value of $\not{p}_T = 123$ GeV due to neutrinos from the LSP decay. In many studies the effective mass,

$$M_{\text{eff}} = \not{p}_T + \sum p_{\text{jets}}^T, \tag{26}$$

is used to "measure" the effective SUSY mass scale. However, they assume a stable LSP and thus M_{eff} receives a sizable contribution from $\not{p}_T$. Our signatures tend to look softer than those of most R-parity conserving scenarios because some of the decay products of the LSP are not included in the sum in Eq. (26). A useful discriminating variable to increase the significance of our signal could be the scalar sum of missing transverse momentum, all jets, leptons, and hadronic taus,

$$S_T = \not{p}_T + \sum p_{\text{jets}}^T + \sum p_\ell^T + \sum p_{\tau_{\text{had}}}^T. \tag{27}$$

For example, the ratio of Eqs. (26) and (27) is 0.85 for **BP3**.

Finally, it is difficult to constrain the region $M_{1/2} \lesssim 230$ GeV in our model due to the finite lifetime of the LSP, since many supersymmetry searches only reconstruct leptons and jets which originate from the primary vertex. We thus conclude that allowing events with displaced vertices would certainly be advantageous to establish bounds in the low $M_{1/2}$ region.

ACKNOWLEDGMENTS

We thank H. K. Dreiner, C.-H. Kom and A. Williams for useful discussions. J. S. K. thanks the University of Bonn and the Bethe Center for Theoretical Physics for hospitality during numerous visits. M. H. thanks the University of Adelaide for hospitality during her visit. This work is supported in part by the Deutsche Telekom Stiftung, by the Bonn-Cologne Graduate School of Physics, and by the ARC Centre of Excellence for Particle Physics at the Terascale.

[1] H. E. Haber and G. L. Kane, Phys. Rep. **117**, 75 (1985).
[2] M. Drees, R. Godbole, and P. Roy, in *Theory and Phenomenology of sparticles: An Account of Four-Dimensional $N = 1$ Supersymmetry in High Energy Physics* (World Scientific, Hackensack, NJ, 2004), p. 555.
[3] G. Aad *et al.* (ATLAS Collaboration), Phys. Lett. B **710**, 67 (2012).
[4] G. Aad *et al.* (ATLAS Collaboration), J. High Energy Phys. 11 (2011) 099.
[5] Atlas Collaboration, *Conference Note from the 47th Rencontres de Moriond on QCD and High Energy Interactions, La Thuile, Italy, 2012* (Report No. ATLAS-CONF-2012-033), https://cdsweb.cern.ch/record/1432199 (unpublished).
[6] CMS Collaboration, Report No. CMS-PAS-SUS-11-005, http://cdsweb.cern.ch/record/1377032 (unpublished).
[7] CMS Collaboration, Report No. CMS-PAS-SUS-11-004, http://cdsweb.cern.ch/record/1378478 (unpublished).
[8] S. Chatrchyan *et al.* (CMS Collaboration), Phys. Rev. Lett. **107**, 221804 (2011).
[9] G. Aad *et al.* (ATLAS Collaboration), Phys. Rev. D **85**, 012006 (2012).

[10] Atlas Collaboration, in *47th Rencontres de Moriond on QCD and High Energy Interactions, La Thuile, Italy, 2012* (Report No. ATLAS-CONF-2012-041), https://cdsweb.cern.ch/record/1435195 (unpublished).

[11] CMS Collaboration, Report No. CMS-PAS-SUS-11-015, http://cdsweb.cern.ch/record/1380922 and updated plots at https://twiki.cern.ch/twiki/bin/view/CMSPublic/PhysicsResultsSUS12010 (unpublished).

[12] G. Aad *et al.* (ATLAS Collaboration), Phys. Lett. B **709**, 137 (2012).

[13] CMS Collaboration, Report No. CMS-PAS-SUS-11-011, http://cdsweb.cern.ch/record/1370065 and updated plots for 5 inv fb at https://twiki.cern.ch/twiki/bin/view/CMSPublic/PhysicsResultsSUS110115fb (unpublished).

[14] CMS Collaboration, Report No. CMS-PAS-SUS-11-010, http://cdsweb.cern.ch/record/1370064 and updated plots for 5 inv fb at https://twiki.cern.ch/twiki/bin/view/CMSPublic/PhysicsResultsSUS110105fb (unpublished).

[15] G. R. Farrar and P. Fayet, Phys. Lett. B **76**, 575 (1978).

[16] H. K. Dreiner, Pramana J. Phys., **51**, 123 (1998).

[17] H. K. Dreiner, C. Luhn, and M. Thormeier, Phys. Rev. D **73**, 075007 (2006).

[18] H.-B. Kim and J. E. Kim, Phys. Lett. B **527**, 18 (2002).

[19] W. Buchmuller, L. Covi, K. Hamaguchi, A. Ibarra, and T. Yanagida, J. High Energy Phys. 03 (2007) 037.

[20] H. K. Dreiner and S. Grab, AIP Conf. Proc. **1200**, 358 (2010).

[21] K. Desch, S. Fleischmann, P. Wienemann, H. K. Dreiner, and S. Grab, Phys. Rev. D **83**, 015013 (2011).

[22] H. K. Dreiner, S. Grab, and T. Stefaniak, Phys. Rev. D **84**, 035023 (2011).

[23] B. C. Allanach and C. H. Kom, J. High Energy Phys. 04 (2008) 081.

[24] H. K. Dreiner, M. Hanussek, and S. Grab, Phys. Rev. D **82**, 055027 (2010).

[25] H. K. Dreiner, M. Hanussek, J. S. Kim, and C. H. Kom, Phys. Rev. D **84**, 113005 (2011).

[26] H. K. Dreiner, J. S. Kim, and M. Thormeier, arXiv:0711.4315.

[27] R. N. Mohapatra and G. Senjanovic, Phys. Rev. Lett. **44**, 912 (1980).

[28] P. Minkowski, Phys. Lett. B **67**, 421 (1977).

[29] Atlas Collaboration, Report No. ATLAS-CONF-2012-001, https://cdsweb.cern.ch/record/1418920 (unpublished).

[30] Atlas Collaboration, Report No. ATLAS-CONF-2012-035, https://cdsweb.cern.ch/record/1432202 (unpublished).

[31] S. Chatrchyan *et al.* (CMS Collaboration), arXiv:1204.5341.

[32] P. W. Graham, D. E. Kaplan, S. Rajendran, and P. Saraswat, arXiv:1204.6038.

[33] S. Chatrchyan *et al.* (CMS Collaboration), Phys. Lett. B **704**, 411 (2011).

[34] G. Aad *et al.* (ATLAS Collaboration), Phys. Lett. B **707**, 478 (2012).

[35] G. Aad *et al.* (ATLAS Collaboration), Eur. Phys. J. C **71**, 1809 (2011).

[36] H. K. Dreiner and T. Stefaniak, arXiv:1201.5014 [Phys. Rev. D (to be published)].

[37] M. Hirsch, M. A. Diaz, W. Porod, J. C. Romao, and J. W. F. Valle, Phys. Rev. D **62**, 113008 (2000); **65**, 119901(E) (2002).

[38] B. C. Allanach, A. Dedes, and H. K. Dreiner, Phys. Rev. D **69**, 115002 (2004); **72**, 079902 (2005).

[39] S. Weinberg, Phys. Rev. Lett. **43**, 1566 (1979).

[40] N. Sakai and T. Yanagida, Nucl. Phys. **B197**, 533 (1982).

[41] S. Weinberg, Phys. Rev. D **26**, 287 (1982).

[42] H. K. Dreiner and M. Thormeier, Phys. Rev. D **69**, 053002 (2004).

[43] E. Nardi, Phys. Rev. D **55**, 5772 (1997).

[44] L. J. Hall and M. Suzuki, Nucl. Phys. **B231**, 419 (1984).

[45] N. Cabibbo, Phys. Rev. Lett. **10**, 531 (1963).

[46] M. Kobayashi and T. Maskawa, Prog. Theor. Phys. **49**, 652 (1973).

[47] Y. Grossman and H. E. Haber, Phys. Rev. D **59**, 093008 (1999).

[48] Because of the antisymmetry of λ_{ijk}, $\lambda_{333} = 0$ and ℓ_3 could only contribute to neutrino masses via λ_{233}. This means that for a sizable contribution, ℓ_3 must be several orders of magnitude larger than ℓ_1 or ℓ_2.

[49] T. Schwetz, M. Tortola, and J. W. F. Valle, New J. Phys. **13**, 063004 (2011).

[50] F. P. An *et al.* (DAYA-BAY Collaboration), Phys. Rev. Lett. **108**, 171803 (2012).

[51] J. K. Ahn *et al.* (RENO Collaboration), arXiv:1204.0626.

[52] B. C. Allanach, C. H. Kom, and M. Hanussek, Comput. Phys. Commun. **183**, 785 (2012).

[53] F. James and M. Roos, Comput. Phys. Commun. **10**, 343 (1975).

[54] ℓ_3 has no relevance for the collider signatures as long as it does not become several orders of magnitude larger than ℓ_1 and ℓ_2.

[55] R. Barbier *et al.*, Phys. Rep. **420**, 1 (2005).

[56] H. K. Dreiner, M. Kramer, and B. O'Leary, Phys. Rev. D **75**, 114016 (2007).

[57] In principle, any sparticle could here be the LSP in $\not{R}_p$ models since it is unstable, [20]. However, since the L-violating couplings in the hierarchical B_3 cMSSM are small, the particle spectrum remains very similar to the R_p cMSSM and thus the lighter stau is always the lightest sfermion due to large left-right mixing.

[58] Only in a small part of the neutralino LSP region, where $M_{1/2} \lesssim 240$ GeV, the lifetime of the LSP can become larger than $c\tau \gtrsim 15$ mm.

[59] F. E. Paige, S. D. Protopopescu, H. Baer, and X. Tata, arXiv:hep-ph/0312045.

[60] W. Porod and F. Staub, arXiv:1104.1573.

[61] A. Sherstnev and R. S. Thorne, Eur. Phys. J. C **55**, 553 (2008).

[62] G. Corcella, I. G. Knowles, G. Marchesini, S. Moretti, K. Odagiri, P. Richardson, M. H. Seymour, and B. R. Webber, J. High Energy Phys. 01 (2001) 010.

[63] W. Beenakker, R. Hopker, and M. Spira, arXiv:hep-ph/9611232.

[64] S. Ovyn, X. Rouby, and V. Lemaitre, arXiv:0903.2225.

[65] R. Brun and F. Rademakers, Nucl. Instrum. Methods Phys. Res., Sect. A **389**, 81 (1997).

[66] W. A. Rolke, A. M. Lopez, and J. Conrad, Nucl. Instrum. Methods Phys. Res., Sect. A **551**, 493 (2005).

[67] Note that additional jets can also arise from QCD Bremsstrahlung.
[68] G. Aad *et al.* (ATLAS Collaboration), arXiv:1203.6580.
[69] G. Aad *et al.* (ATLAS Collaboration), arXiv:1203.6193.
[70] Atlas Collaboration, Report No. ATLAS-CONF-2012-019, http://cdsweb.cern.ch/record/1430033 (unpublished).
[71] S. Chatrchyan *et al.* (CMS Collaboration), arXiv:1202.1488.
[72] U. Ellwanger, C. Hugonie, and A. M. Teixeira, Phys. Rep. **496**, 1 (2010).
[73] D. A. Vasquez, G. Belanger, C. Boehm, J. Da Silva, P. Richardson, and C. Wymant, arXiv:1203.3446.
[74] U. Ellwanger and C. Hugonie, arXiv:1203.5048.